Impact of Air-to-Air Heat Pumps on Energy and Climate in a Mid-Latitude City

David Meyer[1] (ORCID: 0000-0002-7071-7547)

Robert Schoetter[2] (ORCID: 0000-0002-2284-4592)

Maarten van Reeuwijk[1] (ORCID: 0000-0003-4840-5050)

[1]Department of Civil and Environmental Engineering, Imperial College London, London, UK

[2]CNRM, Université de Toulouse, Météo-France, CNRS, Toulouse, France

Correspondence to David Meyer (email: d.meyer@imperial.ac.uk)

Keywords: heat pumps, building energy consumption, decarbonisation, urban climate

Abstract

Exploring the potential effects of transitioning entirely to air-to-air heat pumps (AAHPs), we use an integrated weather and heat pump model to understand their performance across several building and weather conditions in Toulouse, France. In central Toulouse, where electric and gas heating are similarly adopted, a shift to AAHPs cuts annual electric consumption. Yet, during colder periods, a drop in their efficiency can cause a spike in electricity use. In regions predominantly relying on non-electric heaters, such as gas boilers, introducing AAHPs is expected to increase electricity demand as the heating system transitions to all-electric, though to a lesser extent and with much greater efficiency than traditional systems such as electric resistive heaters. In a separate analysis to evaluate the impact of AAHPs on local climate conditions, we find that AAHPs have a small influence of about 0.5 °C on the outdoor air temperature. This change is thus unlikely to meaningfully alter AAHPs' performance through feedback.

1. Introduction

In 2018, residential space heating made up about 16% of the final energy consumption in the European Union's group of 28 (EUROSTAT, 2020). On a global scale in 2017, this constituted about 10% for most of the largest energy consumers (IEA 2019), representing approximately 7% of total worldwide carbon-dioxide (CO_2) emissions. Heat pumps (HPs) are a promising technology for replacing fossil-fuel-based with high-efficiency electric-based heating (Staffell et al., 2012) to help reduce the energy use and greenhouse gas emissions in buildings (Knobloch et al., 2020; Kozarcanin et al., 2020; Vaishnav & Fatimah, 2020). Their efficiency in reducing CO_2 emissions is however dependent on the type of HP used and the way electricity is produced (Kozarcanin et al., 2020; Lund et al., 2014; Staffell et al., 2015).

Physically, HPs move thermal energy from a cold location (e.g., outdoor air) to a warmer one (e.g., indoor air; Stoecker and Jones, 1982). Depending on where the energy is sourced and released (e.g., in air, ground, or water) several HP types exist (see Staffell et al., 2012). Today, air-to-air HPs (AAHP; Figure 1) are the predominant type sold worldwide (IEA, 2020) and in the EU-21 (EHPA, 2020). As such this is the type examined in our study. Two variables are of main interest in simulating AAHPs: capacity (Q_{capacity}; i.e., the actual amount of thermal energy Q_{heat} that it can provide at a given time of operation) and work (W; i.e., the actual amount of electric energy used to drive the system at a given time of operation). The ratio of thermal energy rejected into the building to that of electric energy used to drive the compressor defines the coefficient of performance (COP, i.e., $\mathrm{COP} = Q_{\mathrm{heat}} / W$), a common metric to rate HPs' efficiency. Although work and capacity (and hence COP) are often used and reported as static parameters, in real systems, these are a function of several factors such as indoor and outdoor conditions and use. In our study, we explicitly model both COP and capacity to better understand the transient behaviour of AAHPs under different building and weather conditions.

In modelling the impact of HPs on building's energy use and greenhouse gas emissions, earlier studies made use of statistical and empirical analyses. For example, Knobloch et al. (2020) analysed current and future HP emissions trade-offs in 59 world regions and found HPs to be less emission intensive than fossil-fuel-based alternatives in 53 regions, with France, the country with the largest share of nuclear power plants in electricity production globally, having the lowest CO_2 emissions. More generally, they found that even if future end-use electrification is not matched by a rapid decarbonization of electricity production, a switch to HPs will likely reduce emissions in almost all world regions. Contrasting this global perspective, Vaishnav and Fatimah's (2020) analysis on how a switch from natural gas to electric heat pumps could impact heating bills, CO_2, and other pollutant emissions in the United States (US), they found that the impact for single family dwellings were negative—i.e., experiencing higher heating bills and increased CO2 emissions—in 658 out of the 883 locations analysed. Furthermore, they identified a notable shift in peak electricity demand patterns and emphasized the potential for a carbon tax to make electric heat pumps both environmentally and economically favourable. While Knobloch et al. (2020) provide a global perspective incorporating diverse energy landscapes across 59 regions, Vaishnav and Fatimah (2020) focus solely on the US, emphasizing the economic and peak demand implications, and the potential effects of a carbon tax, showcasing the nuances that arise when narrowing the scope from a global to a national analysis. Collectively, these studies highlight the complexities of electrification's environmental and economic trade-offs, underscoring the importance of regional analyses and broader policy considerations.

Within meteorological and urban-climate contexts, building energy models (BEMs) coupled to urban canopy models (UCMs) and numerical weather prediction (NWP) models (e.g. Martilli et al. 2002; Salamanca et al. 2010; Kikegawa et al. 2003; Meyer et al. 2020a) are common tools to investigate the interactions between people, buildings, and atmosphere as they can provide accurate weather conditions (e.g., by accounting for urban heat island effects) to BEMs and allow for the feedback between the two to be explored. Although several meteorological studies (e.g., de Munck et al., 2013; Salamanca et al., 2013), have shown the impact of air conditioning on local temperature and energy use with coupled models, to our knowledge, none have so far explored the impact of AAHPs. Here we explore the potential ramifications of adopting AAHPs on the energy dynamics and local climate of Toulouse, France. Our goal is to quantify the shifts in heating energy use, surface energy balance, and ambient temperature that might result from a theoretical transition from fossil fuel-based and resistive heaters to AAHPs. Diverging from previous statistical analyses on HPs, we design and implement numerical models that capture the day-to-day influence of AAHPs with a 250 m spatial granularity across the city, considering a complete year's meteorological conditions.

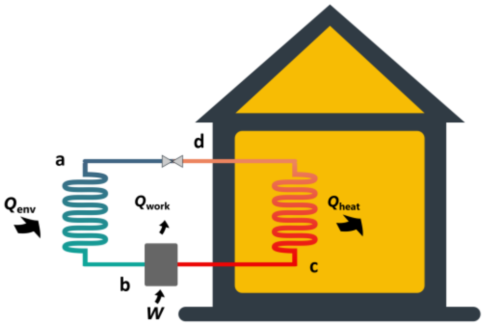

Figure 1 | Schematic of the vapour–compression refrigeration cycle used by an electrically driven AAHP and as implemented in this study. (**a**) The refrigerant absorbs thermal energy (Q_{env}) from the environment through the external coil. (**b**) This low-pressure, low-temperature refrigerant then moves to the compressor where work (W) is done to increase its pressure and temperature. (**c**) The now high-pressure, high-temperature refrigerant moves to the indoor coil, where it releases its thermal energy (Q_{heat}) to heat the indoor air inside the building through the internal coil. (**d**) Following this heat release, the refrigerant, still under high pressure but now at a lower temperature, passes through the expansion valve, where its pressure decreases, readying it to absorb heat from the environment once more, thereby continuing the cycle.

2. Methods

2.1 Modelling Approach

To lay the foundation for our study, we begin by defining a baseline scenario based on the work by Schoetter et al. (2017a). Their work provides a detailed simulation of building energy use for Toulouse between March 2004 to February 2005. It is chosen as (i) it offers a high-resolution snapshot of building energy use in Toulouse, both spatially (at 250 m) and temporally (daily) and, (ii) it has undergone meticulous scrutiny and evaluation, ensuring its reliability. This baseline serves as a reference model of the heating systems present in Toulouse during the 2004-2005 timeframe, with all variables and configurations precisely mirroring those detailed in Schoetter et al. (2017a). Our analysis then encompasses four distinct AAHP scenarios, each representing a varying rated COP (RC), denoting the COP at standard conditions as specified by the manufacturers. While these RC values, set at 2.0, 2.5, 3.0, and 3.5, serve as a reference, our model dynamically adjusts the actual COP in response to varying conditions like temperature. For each scenario, an independent simulation is performed, which is subsequently compared against the baseline for comparison. To estimate the impact of AAHP on energy use, we undertake offline UCM simulations—i.e., forced with observed meteorological data from the centre of Toulouse. During the summer, AAHPs are repurposed as air conditioners (AC). Lastly, to consider the impact of AAHPs on the microclimate, we integrate the UCM with an atmospheric modelling framework and run it for a particularly cold period between 22 and 30 January 2005.

2.2 Numerical Models

The Town Energy Balance (TEB) model (Masson, 2000) is a physically based UCM used to calculate the exchange of momentum, energy and water between cities and the atmosphere. TEB is available as standalone software (Meyer, Schoetter, Masson, et al.,

2020) or as a component in the EXternalised SURFace SURFEX suite (Masson et al., 2013). Additionally, it is integrated into numerical weather forecasting and research platforms such as Meso-NH (Lemonsu & Masson, 2002) and WRF-TEB through WRF-CMake (Meyer, Schoetter, Riechert, et al., 2020a; Riechert & Meyer, 2019). In this study, we use SURFEX-TEB version 8.2 (Schoetter et al., 2017b) as described in Schoetter et al. (2017a). SURFEX-TEB computes the urban surface energy budget (net radiation, turbulent sensible and latent heat flux, and storage heat flux) as a function of meteorological forcing (air temperature and humidity, wind speed, downwelling solar and terrestrial radiation, and precipitation rate) by assuming a simplified street canyon geometry. The energy budget of a representative building at district scale (e.g. 250 m^2) is solved to compute the indoor air temperature, humidity, and building energy use as a function of the simulated meteorological conditions, physical characteristics of the building envelope (e.g. roof and wall materials, windows), and human behaviour related to the building energy use (Bueno et al., 2012; Pigeon et al., 2014). Finally, the surface boundary layer scheme of Hamdi and Masson (2008) is used to calculate vertical profiles of the meteorological variables in the urban roughness sublayer. The model allows to simulate realistic values of outdoor and indoor air temperature and humidity and use them as boundary conditions to the AAHP model. To simulate AAHPs, we couple MinimalDX version 0.1.4 (Meyer & Raustad, 2020)—a simplified single-speed, direct-expansion (DX) coil model from Energy Plus (Crawley et al., 2001)—to TEB and SURFEX-TEB. MinimalDX allows the investigation of a change in performance as a function of indoor and outdoor conditions using bivariate quadratic fits to model the capacity and the electric input ratio (EIR = 1/COP) as a function of indoor wet bulb temperature and outdoor dry bulb temperature. These curves are either generated for a specific HP or air conditioning (AC) model and make, or for more general classes (e.g., domestic or residential split type AC unit; Cutler et al., 2013). MinimalDX is configured with performance and capacity curves from Cutler et al. (2013). In this study, we investigate various scenarios with rated COP (RC) values such as 2, 2.5, 3, and 3.5. This range is based on prior studies indicating that under realistic conditions, the COP typically falls between 3 and 3.5 (Staffell et al., 2012). In modelling HPs, we did not consider the influence of internal fans on the energy use or heat gains given their large variability between systems and their overall small impact. To account for defrost operation, we set a resistive defrost strategy at 20% of the total rated capacity. The design temperature for heating is specified as a function of building use and socio-demographical indicators exactly as described in Schoetter et al. (2017a) for both baseline and RC scenarios. However, a change is made between baseline and RC scenarios for the capacity of the heating system (from 3.23 GW as in Schoetter et al., 2017a to 6.64 GW). Schoetter et al. (2017a) limited the capacity to a degree that the heating design temperature is only maintained for outdoor temperature above 10 °C. This parametrises both limited heating system capacity and the fact that inhabitants limit heating during cold spells to avoid excessive energy bills. This setting is maintained for the baseline, but not for RC scenarios where this limitation is removed since we assume that HPs are designed with sufficient capacity and because of reduced energy use, inhabitants no longer try to limit energy use during cold spells (rebound effect, see more in the Conclusion). For ACs, Schoetter et al. (2017a) considered only very weak usage since this corresponds to their evaluation period of March 2004 to March 2005 in Toulouse when AC was nearly inexistent. Here, we change the AC design temperature for RC scenarios to consider a more systematic deployment of ACs and thus enable the investigation of rebound effects in the summer. The design temperature is 26°C (30°C) in occupied (vacant) residential, commercial, and office buildings and 26°C in hospitals. Buildings with other uses (agriculture, castle, industrial, religious, educational, sports) are assumed to be without ACs. To compute the fraction of internal heat gains we account for a variable fraction of internal heat gains associated with electricity based on the outdoor air temperature to range between 0.7 (as reported in Bueno et al., 2012) in the winter and 1 in the summer where gas use is assumed near zero. This is computed as $0.7 + 0.3\,\frac{(T_t - T_{\min})}{(T_{\max} - T_{\min})}$ with T_t the temperature at time t, and $T_{\min}$ and $T_{\max}$ the minimum and maximum temperature over the whole period respectively. For online simulations to consider the impact of AAHPs on the microclimate during a cold period between 22 and 30 January 2005, we use the atmospheric model Meso-NH version 5.3—a mesoscale, anelastic, nonhydrostatic model (Lac et al., 2018; Lafore et al., 1998). The model is run coupled to SURFEX-TEB-MinimalDX and configured for baseline and RC@2.5 scenarios as described earlier. For initialisation and forcing we use the European Centre for Medium-Range Weather Forecasts (ECMWF) high-resolution operational analysis data. We run the model with two-way grid nesting from outermost to innermost 250 m resolution domain between 20 and 30 January 2005 but report results for the cold spell period between 22 and 30 January 2005 to allow for spin-up. Other settings are as reported in Kwok et al. (2021).

2.3 Domain of Investigation

Toulouse is the fourth largest city in France, with 475,438 inhabitants (INSEE, 2016) in its main municipality. It experiences relatively mild winters with prevailing air temperature mostly between 0 and 15 °C (Joly et al., 2010). Simulations are conducted for a 15 x 15 km domain at 250 m horizontal resolution covering most of Toulouse (Figure 2b) between March 2004 and February 2005 as (i) meteorological parameters for TEB from the CAPITOUL campaign (Masson et al., 2008) are available for this period and, (ii) inventory of building energy use to evaluate the simulated building energy use are available from Pigeon et al. (2007). Urban morphology data such as buildings' plan area, density, and height are from Bocher et al. (2018). Building construction and insulation materials are from Tornay et al. (2017). Heating system types are available from the French institute for statistics and economics (INSEE) at the scale of administrative areas comprising of approximately 2,000 individuals and account for the following fractions (weighted by building volume; Figure S3): electric (resistive heaters) 52.3%, natural gas 41%, wood 4.4%, and oil 2.3%. It is assumed that for a given administrative area, all buildings are heated with the average share of heating system types, thus neglecting potential correlations between heating system type and building use or size.

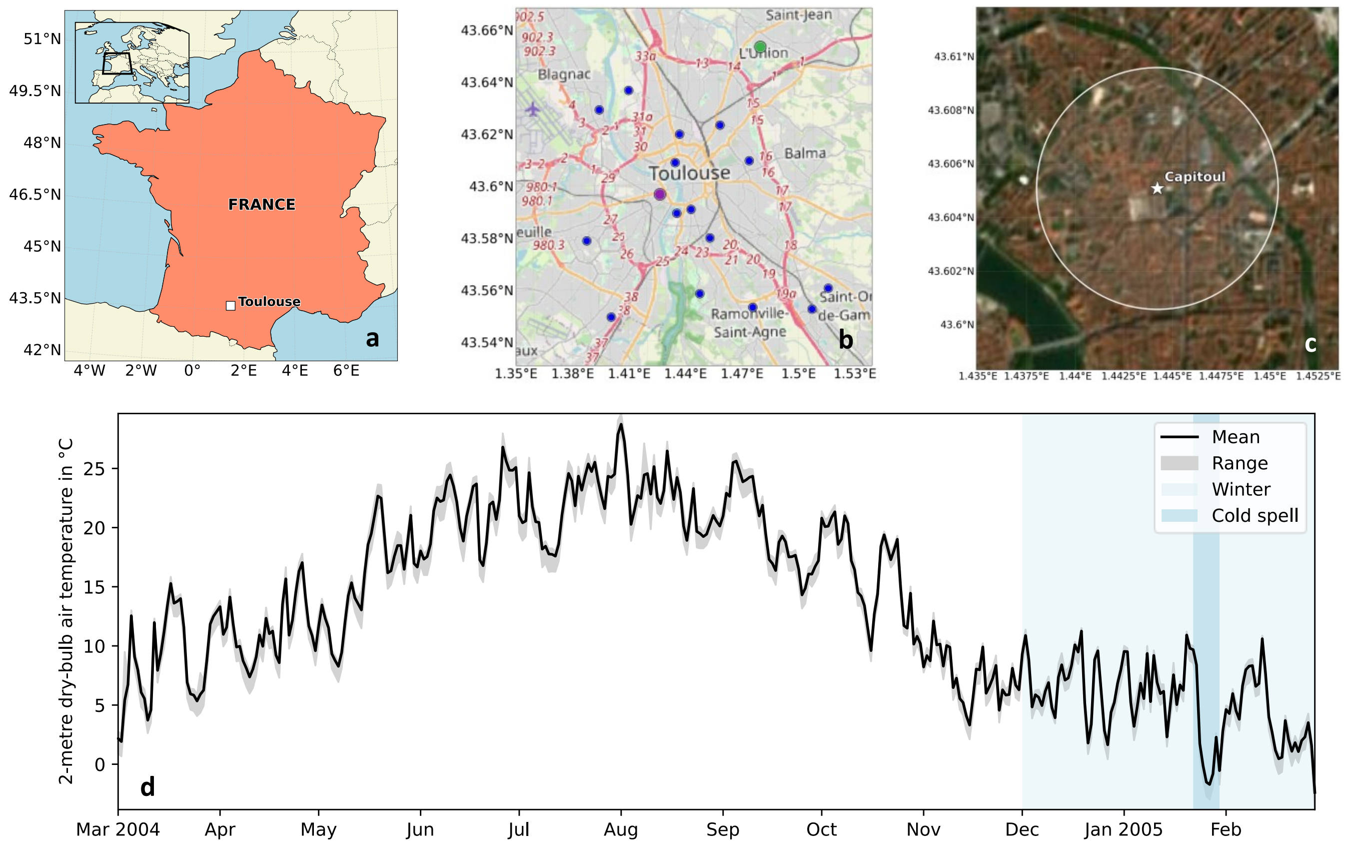

Figure 2 | Investigation domain and time-period used in the simulations. (**a**) The location of Toulouse is shown relative to France and mainland Europe (inset). (**b**) The simulation domain with 17 weather stations is shown by blue circles; the larger purple and green circles show the stations closest to (Saint Cyprien) and furthest away from (L'Union) the centre of Toulouse. (**c**) The inner-city of Toulouse (i.e., Capitoul) used to evaluate the electric energy use is shown with a white circle. (**d**) Observed daily averaged 2 m air temperature in Toulouse is shown for the simulation period between March 2004 and February 2005. Offline simulations are conducted for the winter period from December 2004 to February 2005. Online simulations are conducted for the cold spell between 22 and 30 January 2005 to estimate the impact of AAHPs on the local microclimate.

3. Results and Discussion

3.1 Energy Use

We begin our investigation by outlining results for the simulated daily building energy use in gigawatt day (GWd; Figure 3; Table 1 BE) for the entire domain as shown in Figure 2b. Simulations are conducted using SURFEX-TEB-MinimalDX offline. The baseline scenario is based on and matches that of Schoetter et al. (2017a; Figure S2). The four specific RC scenarios (namely, RC@2.0, RC@2.5, RC@3.0, RC@3.5) examine a total shift to AAHPs from the baseline scenario at varying rated COP (RC) values. The actual COP is computed by the HP model MinimalDX, while RC values represent the COP under standard conditions (see Methods). The annual building energy use is about 190 GWd (Figure 3c; Table 1) of which 186 GWd is used for heating and 4 GWd for cooling as air conditioning was virtually absent in Toulouse in 2004 (Pigeon et al., 2007). Heating is strongly influenced by the outdoor air temperature, peaking at over 2 GWd during the cold spell (Figure 3b). In the average AAHP scenario, here taken as 2.5 (RC@2.5), annual building heating energy use decreases by 62 % (from 186 to 71 GWd; Table 1). The lower RC@2.0 and upper RC@3.5 scenarios show reductions between 52% and 72%, respectively (Table 1). The building energy use for cooling increases by 169% (from 4 to 11 GWd) because of rebound effects (see Methods). The time series of daily building energy use (Figure 3a) shows a similar trend with savings of over 1.25 GWd in the coolest periods when demand is at its highest.

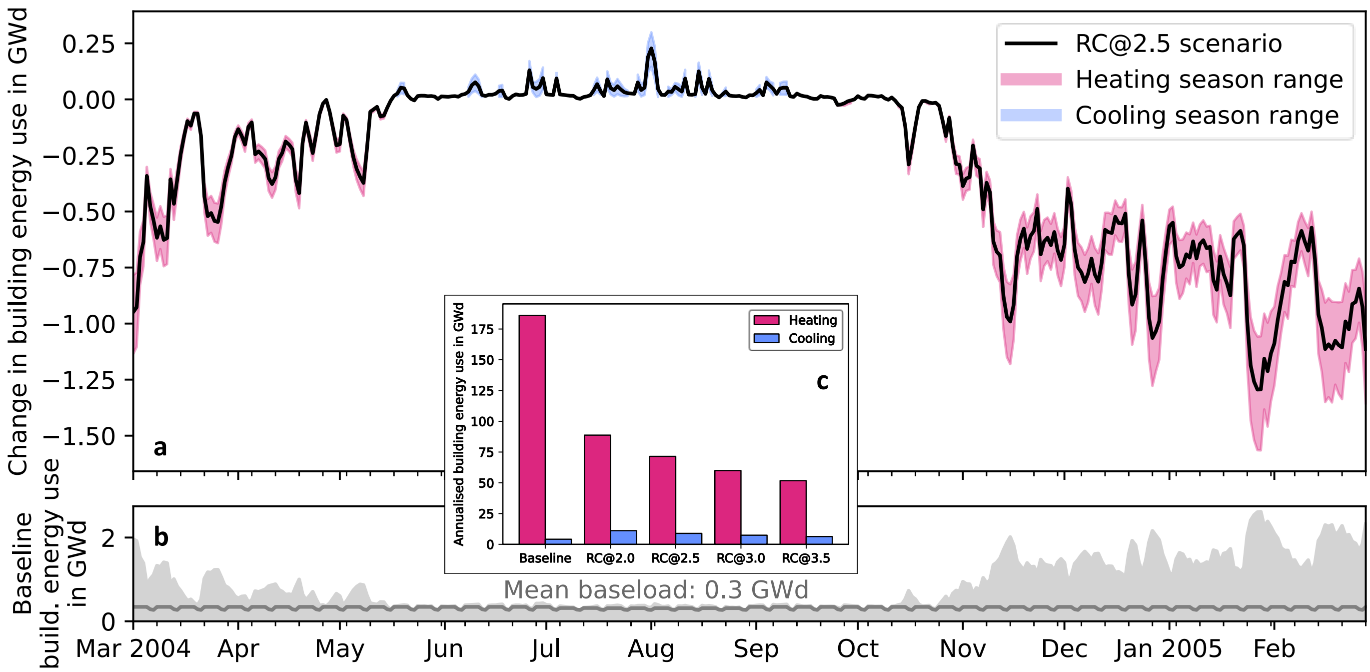

Figure 3 | Energy use differences from a switch to AAHP. (**a**) Timeseries of building energy use for the yearlong simulation showing the (**a**) daily averaged change in building energy use compared to the baseline, (**b**) baseline daily averaged building energy use (shading) and mean baseload (line), (**c**) annual energy use over the entire year (simulation period) for heating and cooling.

Table 1 | Annual heating and cooling energy use. BE: the entire simulation domain for building energy use as in (Figure 3c); $EE_{Capitoul}$: the centre of Toulouse for electric energy only (Figure 4c); EE: the entire simulation domain for electric energy only (Figure 5c). *For cooling EE is the same as BE as all space cooling is already assumed to be provided by electrically driven air conditioning.

	Heating			Cooling		Heating and Cooling		
	BE	$EE_{Capitoul}$	EE	BE (or EE*)	$EE_{Capitoul}$	BE	$EE_{Capitoul}$	EE
	GWd (%)	MWd (%)	GWd (%)	GWd (%)	MWd (%)	GWd (%)	MWd (%)	GWd (%)
Baseline	*186*	*2.4*	*78*	*4*	*0.3*	*190*	*2.7*	*82*
RC@2.0	89 (-52)	2.3 (-6)	89 (14)	11 (169)	0.6 (106)	100 (-48)	2.9 (7)	100 (22)
RC@2.5	71 (-62)	1.9 (-24)	71 (-8)	9 (115)	0.5 (64)	80 (-58)	2.4 (-14)	80 (-2)
RC@3.0	60 (-68)	1.6 (-36)	60 (-23)	7 (79)	0.4 (37)	67 (-65)	2.0 (-28)	67 (-18)
RC@3.5	52 (-72)	1.3 (-45)	52 (-33)	6 (54)	0.4 (17)	58 (-69)	1.7 (-38)	58 (-29)

While building energy use captures the total energy buildings use, transitioning to AAHPs removes the need of gas as a heating fuel. Therefore, our analysis proceeds by focusing solely on the electric energy component across the four scenarios. We assess our energy disaggregation against a prior assessment by Bueno et al. (2012), focusing on Toulouse's centre (Figure 4 and Table 1 $EE_{Capitoul}$) where observational data is present and find consistent results (Figure S4). With electric resistive heaters accounting for roughly 60% of the heating in Toulouse's centre (Figure S3b), baseline estimates for electric use are 2.4 MWd for heating and 0.3 MWd for cooling (Figure 4 and Table 1 $EE_{Capitoul}$). Across all scenarios, the annual electric energy use for heating declines, while it rises for cooling. The combined yearly electric energy use for both heating and cooling reveals an uptick in the RC@2.0 scenario, whereas it drops in the other scenarios. Looking at daily shifts in electric use throughout the year, we notice fluctuations (Figure 4a). These are influenced not just by temperature-related demand, as seen with conventional heating methods, but also by the dynamic capacity of AAHPs, which changes based on both external and internal conditions. For the RC@2.5 scenario, the actual COP dips below 1.5 on multiple occasions during the coldest winter segments (Figure S8).

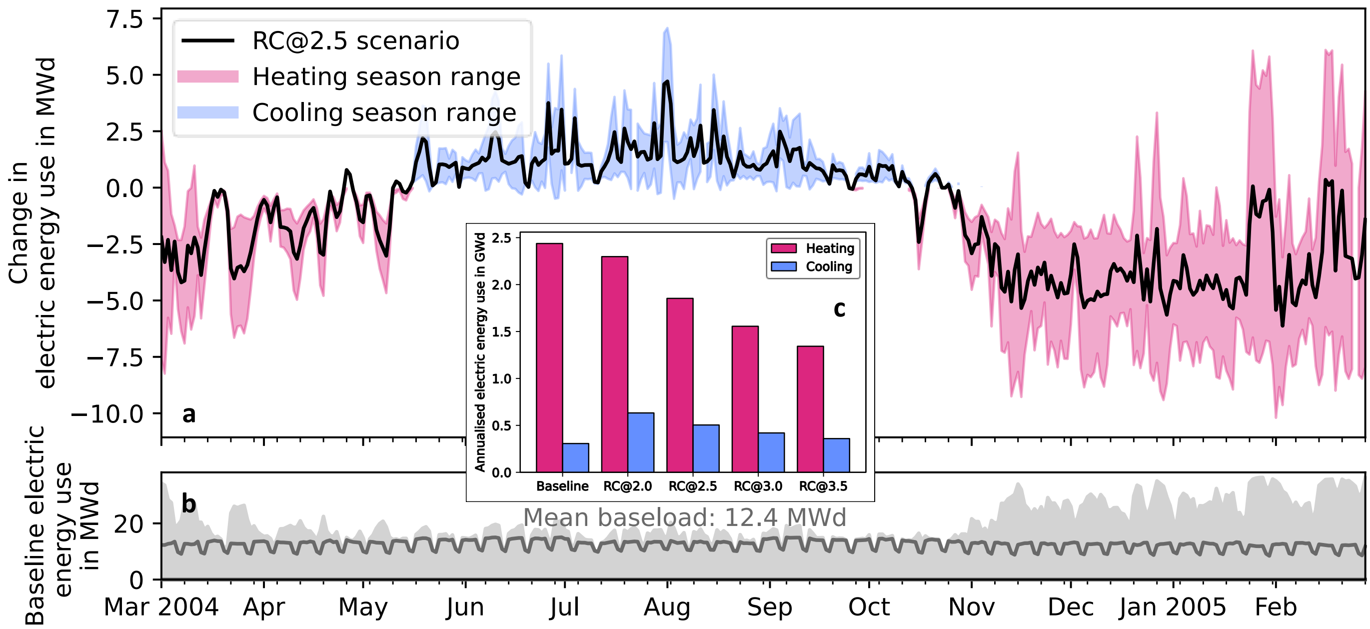

Figure 4 | As Figure 3 but for *electric energy fraction* and inner-city area only shown with a white circle in Figure 2c.

Under the assumption that our modelling technique and energy disaggregation are valid across Toulouse, we extend our analysis to span the full simulation domain. Here, electric resistive heaters are responsible for 52% of Toulouse's heating energy (Figure S3a), projecting a baseline electric energy use of 78 GWd for heating and 4 GWd for cooling (Figure 5 and Table 1 EE). Notably, even with substantial differences between the central and outer regions (Figure S1), our overarching conclusions align closely with those derived from its centre. However, if we were to assess individual grid points rather than average figures for the entire area, marked discrepancies are anticipated. For the RC@2.5 scenario, there is an annual energy reduction of 7 GWd or 8% for heating—a stark contrast to the 24% when analysing just Toulouse's central region, a disparity influenced by the lesser prevalence of resistive heaters and reduced population density (Figure S1).

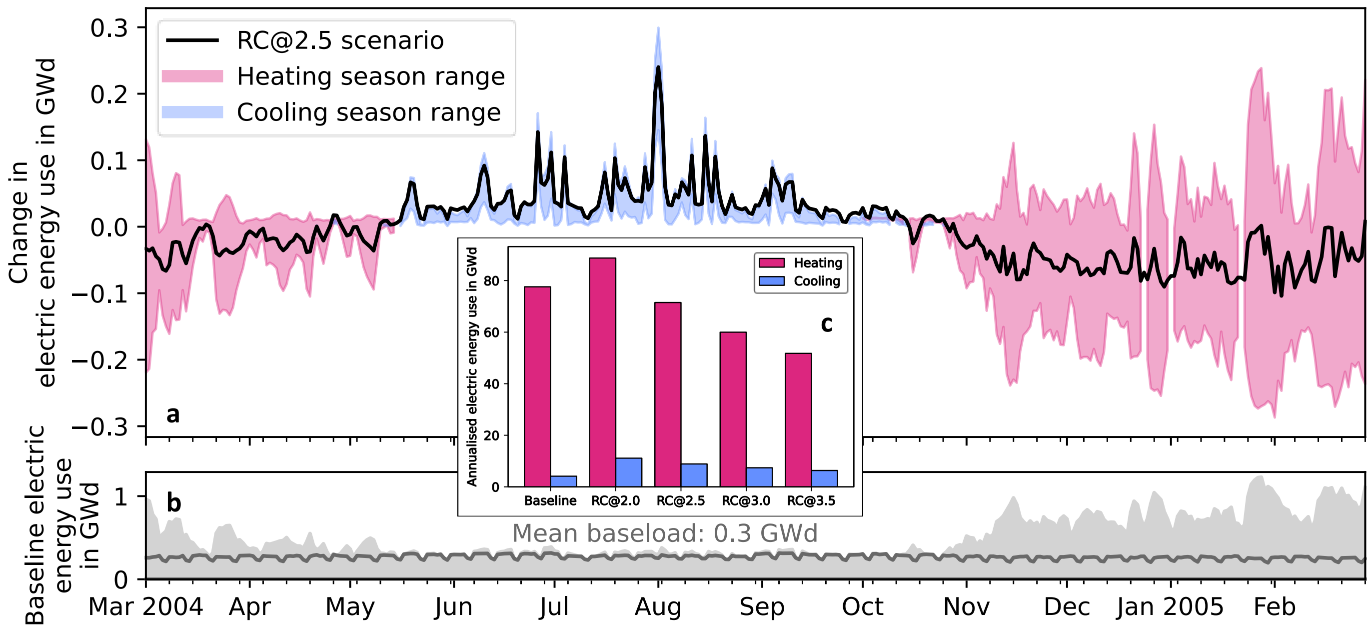

Figure 5 | As figure 4, but for the *whole* simulation domain shown in figure 2b.

3.2 Heat Flux Density

Winter-averaged heat flux densities, both sensible and anthropogenic derived from building energy use, are shown in Figure 6 for the months December to February. Results are produced using the offline SURFEX-TEB-MinimalDX models, comparing the baseline to the RC@2.5 scenario. Central areas show the highest values due to extensive heated floor areas and older building characteristics, such as reduced insulation (Figure S1). In the baseline, values of anthropogenic heat flux peak at over 80 W m^{-2} in some regions and reduce by up to 80% for the AAHP scenario (Figure 3c) given the superior efficiency of AAHPs compared to conventional heating systems. Figures 6d and 6e show the average winter sensible heat flux for baseline and AAHP scenarios. The distribution of this heat flux closely mirrors heating energy use patterns. This is especially marked in winter due to lower solar radiation, making anthropogenic heat flux a key component of the urban energy balance. Within the city centre, AAHPs decrease the sensible heat flux density by between 30 to 40 W m^{-2} (Figure 6f)—notable when total values peak at about 50 W m^{-2}.

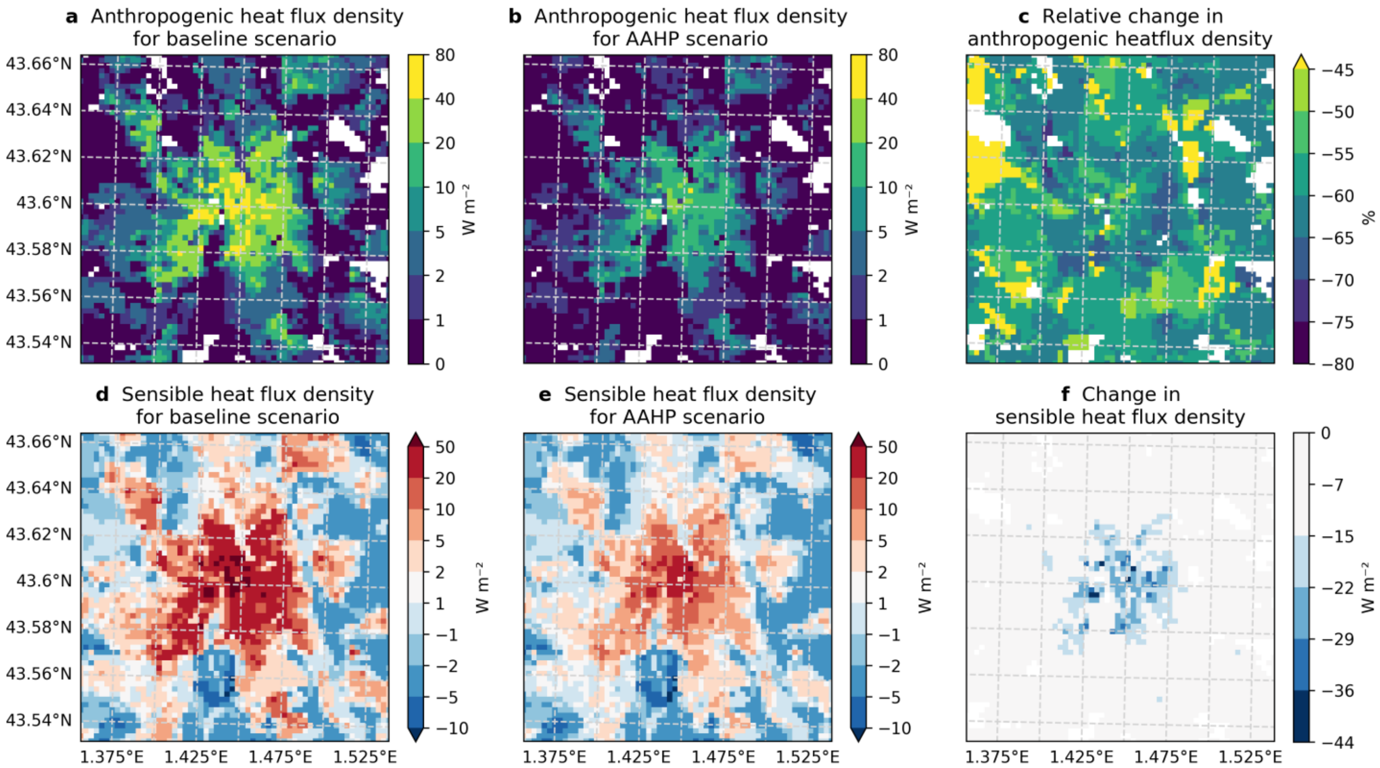

Figure 6 | Spatial variation in anthropogenic and sensible heat flux for the winter under RC@2.5 scenario. Average for December, January, February of (**a**) anthropogenic heat flux due to building energy use (with heating systems in place in 2004 as natural gas, electricity, wood-burning, oil; Figure S1), (**b**) same as (a) but with all heating systems replaced by air-to-air heat pumps, and (**c**) relative difference between (b) and (a). (**d**) and (**e**): same as (a) and (b), but for the sensible heat flux. (**f**) absolute difference between (e) and (d).

3.3 Surface Air Temperature

Using the online MesoNH-SURFEX-TEB-MinimalDX model, we examine the influence of AAHPs on air temperatures at 17 distinct sites (Figure 3b) during the coldest week of 2005 (22-30 January). An evaluation of surface heat flux density shows comparable results between offline and online models (Figure S7). Here, we focus on comparing the baseline to the RC@2.5 scenario. On average, AAHPs change the 2-metre air temperature by less than half a degree (Figure 7). The urban Saint Cyprien station shows, on average the highest difference (Figure 2 & 7; in purple), while more peripheral stations such as L'Union register smaller changes, correlating with smaller variations in heating power and sensible heat fluxes (Figure 6c,f). Daytime and nighttime average 2-metre air temperature variations remain below 0.4°C, with the most substantial deviations found in the city centre.

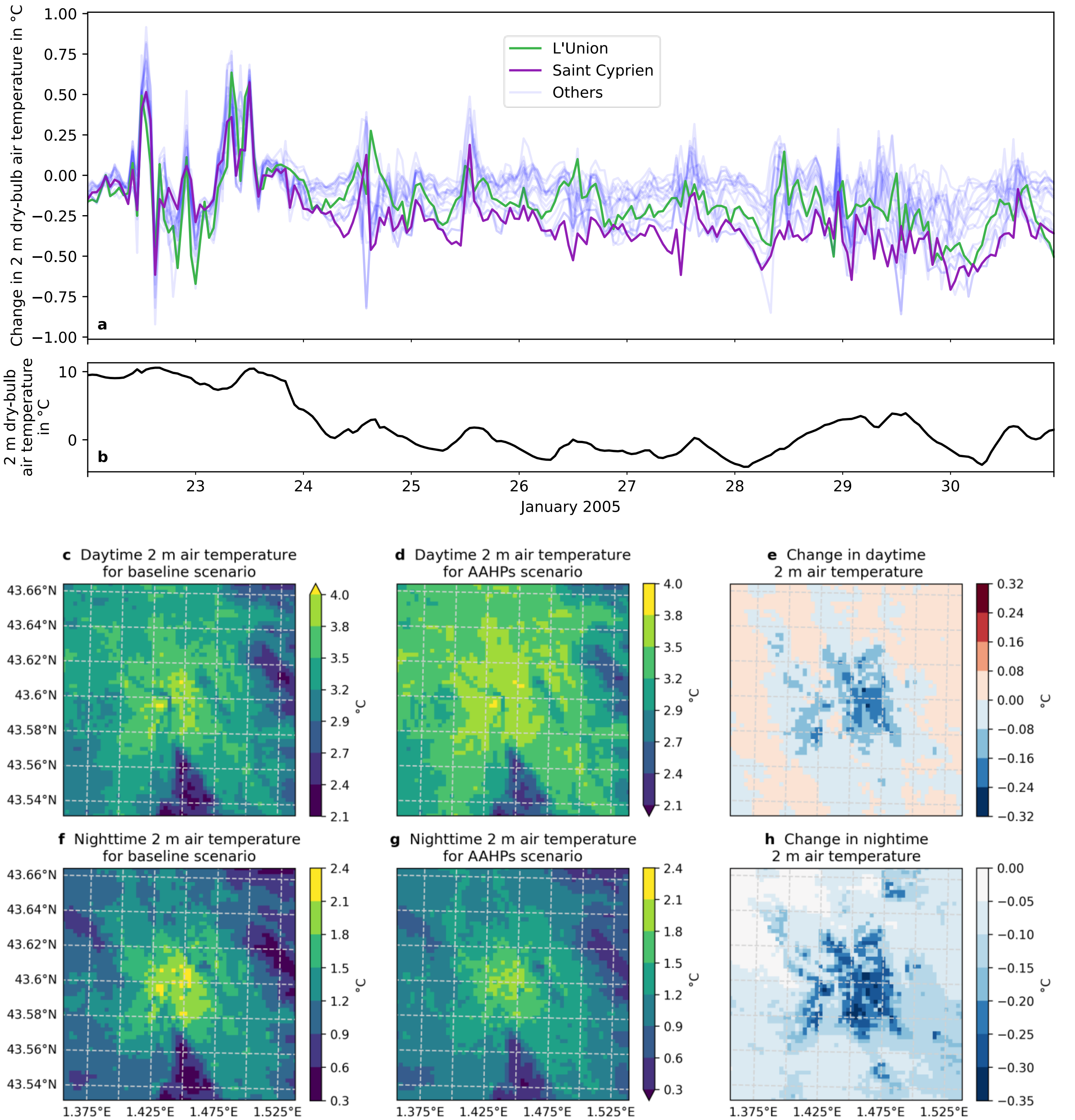

Figure 7 | Change in surface air temperature. (a) Change in 2 m air temperature compared to 17 observational stations, (**b**) average 2 m air temperature from the 17 observational stations, (**c-e**) comparison of daytime 2 m air temperature for baseline (**c**) and AAHP (**d**) scenarios, and (**f-h**) comparison of nighttime 2 m air temperature for baseline (**f**) and AAHP (**g**) scenarios. Differences between baseline and AAHP are illustrated for daytime (**e**) and nighttime (**h**). See Figure S6 for a further comparison of surface air temperature by station.

4. Conclusion

By transitioning to AAHPs, we anticipate reductions in annual building energy use. When looking solely at electricity, there are also predicted savings. However, from the scenarios analysed, large reductions in electricity use are evident with AAHPs when their rated COP is above 2.5 and in areas where electric resistive heaters, being less efficient than heat pumps, constitute about half of the installed heating systems. In areas where gas or other non-electric heating is prevalent, 'savings' manifest as a shift from gas use to electricity demand. In such regions, the existing electrical infrastructure may not be equipped to accommodate this growth, potentially necessitating the construction of new power plants and adjustments of the electricity grid. Conversely, in regions with a substantial proportion of resistive heaters like Toulouse, the existing electrical capacity may already be enough to accommodate a total shift to AAHPs. This nuance holds significant implications for European nations with comparable climates, especially where heating predominantly relies on non-electrical sources like natural gas (EUROSTAT, 2023). Notably, the performance of AAHPs fluctuates in response to local weather conditions, emphasizing its relevance considering the varying energy demands during colder periods. Despite a discernible reduction in sensible heat flux in winter, tempering urban heat island intensity and amplifying cold stress occurrences, our findings suggest the microclimate remains largely unaffected. Across the diverse climates of the EU however, such interactions might yield distinct outcomes, underscoring the importance of region-specific assessments.

The switch to all electric heating reduces direct CO_2 emissions. For the baseline scenario Goret et al (2019) reported up to 100 kg CO_2 m^{-2} for the centre of Toulouse corresponding to districts with high fraction of natural gas heating. Daily local CO_2 emissions due to building heating are zero during the warm season but can reach up to 8 500 tonnes per day during cold spells in winter. Therefore, potential savings in local CO_2 emissions are large for HPs. However, if the electricity consumed by HPs is generated using fossil fuels, indirect CO_2 emissions outside the city may be greater than those produced locally by combustion boilers. Moreover, if the electricity is generated using weather dependent renewable technologies such as wind energy or solar panels, electricity may become unavailable during cold spells or anti cyclonic situations with low wind speed and HPs may overload the power grid. In Toulouse, this may not be an issue at present as the electricity sector in France is dominated by nuclear power (70.6 % in 2019; RTE, 2020) but a switch to weather dependent renewables may result in HPs having a negative impact on the stability of the grid, especially during cold spells.

Current refrigerants used in HPs have high radiative forcing capacity (i.e., a high global warming potential). For example, the most common refrigerant in today's systems is R410-A which has 2000 times the radiative forcing capacity of CO_2. With this there are two potential issues that can be identified: one due to leaks and the other due to end-of-life recycling. For the former, the Intergovernmental Panel on Climate Change (IPCC) estimates that, in developed countries, 1% of a HP's refrigerant is lost to the environment. Therefore, we can estimate that, with the total HP's heating capacity used in the experiment at 6.64 GW and, assuming an average charge of 0.25 kg per kW of capacity (IPCC, 2005), this would correspond to about 33 200 tonnes of CO_2 equivalent per year, or 91 tonnes per day. Compared to the current baseline estimate of 728 040 tonnes for the year from March 2004 to February 2005, or about 2000 tonnes per day, these findings remain below the baseline estimate. For the latter, the IPCC estimates that the refrigerant from a fifth of all HPs is released into the atmosphere rather than being recycled. With this assumption, 664 000 tonnes of CO_2 equivalent would be released at the end of the HPs lifetime, lower than the 728 040 tonnes of CO_2 released annually in the present scenario (March 2004 to February 2005). It is also worth noting that with the introduction of Difluoromethane (R32) refrigerant, this issue will be more than halved given its lower global warming potential of 675 times that of CO_2.

In the realm of heating and air conditioning scenario modelling, it is crucial to consider rebound effects as it can significantly alter our findings. The rebound effect states that as energy efficiency increases, so does energy use due to the reduced cost of usage (Sorrell, 2007). In terms of heating and air conditioning, if the efficiency of these systems is improved, occupants might use them more often, thus offsetting the energy savings. Quantitatively, the rebound effect has been estimated to be about 10-30% for home heating (Greening et al., 2000). Belaïd et al. (2020) found a substantial rebound effect (38 to 86%) for residential electricity use in France, but they did not focus on heat pumps. Gram-Hanssen et al. (2012) found a rebound effect of 20% for AAHPs in Danish residential buildings, due to a higher design temperature, a longer heating period, a larger heated floor area and the potential use of the installed heat pumps as air conditioners. Flower et al. (2020) found evidence for a potential rebound effect for residential buildings in the UK, since a part of the households are restricting their energy use due to the high cost of energy. Furthermore, households who install HPs might use them as air conditioners in the summer and as the climate warms, people will want air conditioning even if they have not had it in the past. In our analysis, we estimate an increase of about 8 GWd (or 13%) over the summer.

From a practical level, we note that the installation of AAHPs may be limited by multiple factors such as noise constraints or local planning restrictions specific to local buildings and typical of some dense historical areas. Similarly, hybrid technology such as solar heat pumps may significantly remove the dependency on the electricity grid. A possible constraint from the use of HPs over fossil fuel technologies or electric resistance heaters is that the capacity and COP decrease with lower outdoor air temperature and may therefore make HPs inefficient during cold spells, possibly when the demand is at its highest. During the cold spell analyzed in online simulations, the drop in temperature resulting from the use of heat pumps accounted for less than half of a degree difference. Such a small difference will not meaningfully change the COP and thus the electricity use and affect the performance by less than 1%. Moreover, these changes tend to be transient as small gradients in air temperature are likely to be quickly carried away by prevailing winds.

While our findings are shaped by certain modelling assumptions and simplifications, they should offer a ballpark estimate of the potential effects and fluctuations from transitioning to AAHPs in a city like Toulouse. Given that our conclusions hinge on factors such as heating capacity, defrost cycle and strategy, and type of system modelled, more in-depth research is warranted to further probe these sensitivities under varied conditions and compare our findings with field studies. In this first effort to quantify the influence of AAHPs through a coupled numerical model, we demonstrate that AAHPs can potentially reduce the aggregate energy use and curb local greenhouse gas emissions in Toulouse when contrasted with prevailing fossil fuel or electric resistive heating systems. However, we anticipate a surge in electric demand during intense cold of winter and peak summer months. This underscores the need of strategic deployment of such technologies to avoid overburdening the electric grid. Our research shows that such flexible physics-based integrated numerical models serve effectively in examining the ramifications of various AAHP scenarios on a broader scale, shedding light on their interplay with a city's energy frameworks and environmental facets.

Author Contributions

Conceptualization: D.M.; Data curation: D.M.; Formal analysis: D.M., R.S.; Investigation: D.M.; Methodology: D.M.; Software: D.M.; Resources: D.M., M.v.R.; Validation: D.M., R.S.; Visualization: D.M.; Writing—original draft preparation: D.M., R.S.; Writing—review & editing: D.M., R.S., M.v.R..

Code and Data Availability

Software, data, and tools are archived with a Singularity (Kurtzer et al., 2017) image deposited on Zenodo as described in the scientific reproducibility section of Meyer et al. (2020b). Users wishing to download or reproduce the results described in this paper can download the archive at https://doi.org/10.5281/zenodo.4009383.

References

Belaïd, F., Youssef, A. B., & Lazaric, N. (2020). Scrutinizing the direct rebound effect for French households using quantile regression and data from an original survey. *Ecological Economics*, *176*, 106755. https://doi.org/10.1016/j.ecolecon.2020.106755

Bocher, E., Petit, G., Bernard, J., & Palominos, S. (2018). A geoprocessing framework to compute urban indicators: The MApUCE tools chain. *Urban Climate*, *24*, 153–174. https://doi.org/10.1016/j.uclim.2018.01.008

Bueno, B., Pigeon, G., Norford, L. K., Zibouche, K., & Marchadier, C. (2012). Development and evaluation of a building energy model integrated in the TEB scheme. *Geoscientific Model Development*, *5*(2), 433–448. https://doi.org/10.5194/gmd-5-433-2012

Crawley, D. B., Lawrie, L. K., Winkelmann, F. C., Buhl, W. F., Huang, Y. J., Pedersen, C. O., Strand, R. K., Liesen, R. J., Fisher, D. E., Witte, M. J., & Glazer, J. (2001). EnergyPlus: Creating a new-generation building energy simulation program. *Energy and Buildings*, *33*(4), 319–331. https://doi.org/10.1016/S0378-7788(00)00114-6

Cutler, D., Winkler, J., Kruis, N., Christensen, C., & Brandemuehl, M. (2013). Improved Modeling of Residential Air Conditioners and Heat Pumps for Energy Calculations. *Office of Scientific and Technical Information (OSTI)*. https://doi.org/10.2172/1067909

de Munck, C., Pigeon, G., Masson, V., Meunier, F., Bousquet, P., Tréméac, B., Merchat, M., Poeuf, P., & Marchadier, C. (2013). How much can air conditioning increase air temperatures for a city like Paris, France? *International Journal of Climatology*, *33*(1), 210–227. https://doi.org/10.1002/joc.3415

EHPA. (2020). *Heat pump sales overview*. http://www.stats.ehpa.org/hp_sales/story_sales/

EUROSTAT. (2020). *Energy consumption in households—Statistics Explained*. https://ec.europa.eu/eurostat/statistics-explained/index.php?title=Energy_consumption_in_households#cite_ref-1

EUROSTAT. (2023). *Energy consumption in households*. https://ec.europa.eu/eurostat/statistics-explained/index.php?title=Energy_consumption_in_households#Energy_consumption_in_households_by_type_of_end-use

Flower, J., Hawker, G., & Bell, K. (2020). Heterogeneity of UK residential heat demand and its impact on the value case for heat pumps. *Energy Policy*, *144*, 111593. https://doi.org/10.1016/j.enpol.2020.111593

Gram-Hanssen, K., Christensen, T. H., & Petersen, P. E. (2012). Air-to-air heat pumps in real-life use: Are potential savings achieved or are they transformed into increased comfort? *Energy and Buildings*, *53*, 64–73. https://doi.org/10.1016/j.enbuild.2012.06.023

Greening, L. A., Greene, D. L., & Di, C. (2000). Energy e$ciency and consumption * the rebound e!ect * a survey. *Energy Policy*.

Hamdi, R., & Masson, V. (2008). Inclusion of a Drag Approach in the Town Energy Balance (TEB) Scheme: Offline 1D Evaluation in a Street Canyon. *Journal of Applied Meteorology and Climatology*, *47*(10), 2627–2644. https://doi.org/10.1175/2008JAMC1865.1

IEA. (2019). Energy Efficiency Indicators Highlights 2019. *Energy Efficiency*, 204.

IEA. (2020). *Heat Pumps – Analysis*. IEA. https://www.iea.org/reports/heat-pumps

INSEE. (2016). *Populations légales 2016—Commune de Toulouse (31555)*. https://www.insee.fr/fr/statistiques/3681328?geo=COM-31555

IPCC (Ed.). (2005). *IPCC/TEAP special report on safeguarding the ozone layer and the global climate system: Issues related to hydrofluorocarbons and perfluorocarbons*. Published for the Intergovernmental Panel on Climate Change [by] Cambridge University Press.

Joly, D., Brossard, T., Cardot, H., Cavailhes, J., Hilal, M., & Wavresky, P. (2010). Les types de climats en France, une construction spatiale. *Cybergeo*. https://doi.org/10.4000/cybergeo.23155

Kikegawa, Y., Genchi, Y., Yoshikado, H., & Kondo, H. (2003). Development of a numerical simulation system toward comprehensive assessments of urban warming countermeasures including their impacts upon the urban buildings' energy-demands. *Applied Energy*, *76*(4), 449–466. https://doi.org/10.1016/S0306-2619(03)00009-6

Knobloch, F., Hanssen, S. V., Lam, A., Pollitt, H., Salas, P., Chewpreecha, U., Huijbregts, M. A. J., & Mercure, J.-F. (2020). Net emission reductions from electric cars and heat pumps in 59 world regions over time. *Nature Sustainability*, *3*(6), 437–447. https://doi.org/10.1038/s41893-020-0488-7

Kozarcanin, S., Hanna, R., Staffell, I., Gross, R., & Andresen, G. B. (2020). Impact of climate change on the cost-optimal mix of decentralised heat pump and gas boiler technologies in Europe. *Energy Policy*, *140*, 111386. https://doi.org/10.1016/j.enpol.2020.111386

Kurtzer, G. M., Sochat, V., & Bauer, M. W. (2017). Singularity: Scientific containers for mobility of compute. *PLOS ONE*, *12*(5), e0177459. https://doi.org/10.1371/journal.pone.0177459

Kwok, Y. T., Schoetter, R., De Munck, C., Lau, K. K.-L., Wong, M. S., & Ng, E. (2021). High-resolution mesoscale simulation of the microclimatic effects of urban development in the past, present, and future Hong Kong. *Urban Climate*, *37*, 100850. https://doi.org/10.1016/j.uclim.2021.100850

Lac, C., Chaboureau, J.-P., Masson, V., Pinty, J.-P., Tulet, P., Escobar, J., Leriche, M., Barthe, C., Aouizerats, B., Augros, C., Aumond, P., Auguste, F., Bechtold, P., Berthet, S., Bielli, S., Bosseur, F., Caumont, O., Cohard, J.-M., Colin, J., … Wautelet, P. (2018). Overview of the Meso-NH model version 5.4 and its applications. *Geoscientific Model Development*, *11*(5), 1929–1969. https://doi.org/10.5194/gmd-11-1929-2018

Lafore, J. P., Stein, J., Asencio, N., Bougeault, P., Ducrocq, V., Duron, J., Fischer, C., Masson, V., Pinty, J. P., Redelsperger, J. L., & Richard, E. (1998). The Meso-NH Atmospheric Simulation System. Part I: adiabatic formulation and control simulations. *Annales Geophysicae*, 20. https://doi.org/10.1007/s00585-997-0090-6

Lemonsu, A., & Masson, V. (2002). Simulation of a Summer Urban Breeze Over Paris. *Boundary-Layer Meteorology*, *104*(3), 463–490. https://doi.org/10.1023/A:1016509614936

Lund, H., Werner, S., Wiltshire, R., Svendsen, S., Thorsen, J. E., Hvelplund, F., & Mathiesen, B. V. (2014). 4th Generation District Heating (4GDH). *Energy*, *68*, 1–11. https://doi.org/10.1016/j.energy.2014.02.089

Martilli, A., Clappier, A., & Rotach, M. W. (2002). An Urban Surface Exchange Parameterisation for Mesoscale Models. *Boundary-Layer Meteorology*, *104*(2), 261–304. https://doi.org/10.1023/A:1016099921195

Masson, V. (2000). A Physically-Based Scheme For The Urban Energy Budget In Atmospheric Models. *Boundary-Layer Meteorology*, *94*(3), 357–397. https://doi.org/10.1023/A:1002463829265

Masson, V., Gomes, L., Pigeon, G., Liousse, C., Pont, V., Lagouarde, J.-P., Voogt, J., Salmond, J., Oke, T. R., Hidalgo, J., Legain, D., Garrouste, O., Lac, C., Connan, O., Briottet, X., Lachérade, S., & Tulet, P. (2008). The Canopy and Aerosol Particles Interactions in TOulouse Urban Layer (CAPITOUL) experiment. *Meteorology and Atmospheric Physics*, *102*(3–4), 135–157. https://doi.org/10.1007/s00703-008-0289-4

Masson, V., Le Moigne, P., Martin, E., Faroux, S., Alias, A., Alkama, R., Belamari, S., Barbu, A., Boone, A., Bouyssel, F., Brousseau, P., Brun, E., Calvet, J.-C., Carrer, D., Decharme, B., Delire, C., Donier, S., Essaouini, K., Gibelin, A.-L., … Voldoire, A. (2013). The SURFEXv7.2 land and ocean surface platform for coupled or offline simulation of earth surface variables and fluxes. *Geoscientific Model Development*, *6*(4), 929–960. https://doi.org/10.5194/gmd-6-929-2013

Meyer, D., & Raustad, R. (2020). MinimalDX. *Zenodo*. https://doi.org/10.5281/zenodo.3892452

Meyer, D., Schoetter, R., Masson, V., & Grimmond, S. (2020). Enhanced software and platform for the Town Energy Balance (TEB) model. *Journal of Open Source Software*, *5*(50), 2008. https://doi.org/10.21105/joss.02008

Meyer, D., Schoetter, R., Riechert, M., Verrelle, A., Tewari, M., Dudhia, J., Masson, V., Reeuwijk, M., & Grimmond, S. (2020a). WRF-TEB: Implementation and evaluation of the coupled Weather Research and Forecasting (WRF) and Town Energy Balance (TEB) model. *Journal of Advances in Modeling Earth Systems*. https://doi.org/10.1029/2019MS001961

Meyer, D., Schoetter, R., Riechert, M., Verrelle, A., Tewari, M., Dudhia, J., Masson, V., van Reeuwijk, M., & Grimmond, S. (2020b). WRF-TEB: Implementation and Evaluation of the Coupled Weather Research and Forecasting (WRF) and Town Energy Balance (TEB) Model. *Journal of Advances in Modeling Earth Systems*, *12*(8). https://doi.org/10.1029/2019MS001961

Pigeon, G., Legain, D., Durand, P., & Masson, V. (2007). Anthropogenic heat release in an old European agglomeration (Toulouse, France). *International Journal of Climatology*, *27*(14), 1969–1981. https://doi.org/10.1002/joc.1530

Pigeon, G., Zibouche, K., Bueno, B., Le Bras, J., & Masson, V. (2014). Improving the capabilities of the Town Energy Balance model with up-to-date building energy simulation algorithms: An application to a set of representative buildings in Paris. *Energy and Buildings*, *76*, 1–14. https://doi.org/10.1016/j.enbuild.2013.10.038

Riechert, M., & Meyer, D. (2019). WRF-CMake: Integrating CMake support into the Advanced Research WRF (ARW) modelling system. *Journal of Open Source Software*, *4*(41), 1468. https://doi.org/10.21105/joss.01468

RTE. (2020). *Bilan électrique 2019*. RTE - Direction innovation et données. https://bilan-electrique-2019.rte-france.com/wp-content/uploads/2020/02/pdf_BE2019.pdf

Salamanca, F., Georgescu, M., Mahalov, A., Moustaoui, M., Wang, M., & Svoma, B. M. (2013). Assessing summertime urban air conditioning consumption in a semiarid environment. *Environmental Research Letters*, *8*(3), 034022. https://doi.org/10.1088/1748-9326/8/3/034022

Salamanca, F., Krpo, A., Martilli, A., & Clappier, A. (2010). A new building energy model coupled with an urban canopy parameterization for urban climate simulations—Part I. formulation, verification, and sensitivity analysis of the model. *Theoretical and Applied Climatology*, *99*(3–4), 331–344. https://doi.org/10.1007/s00704-009-0142-9

Schoetter, R., Masson, V., Bourgeois, A., Pellegrino, M., & Lévy, J.-P. (2017a). Parametrisation of the variety of human behaviour related to building energy consumption in the Town Energy Balance (SURFEX-TEB v. 8.2). *Geoscientific Model Development*, *10*(7), 2801–2831. https://doi.org/10.5194/gmd-10-2801-2017

Schoetter, R., Masson, V., Bourgeois, A., Pellegrino, M., & Lévy, J.-P. (2017b). *Source code and run directories for Schoetter et al., GMD: Parametrisation of the variety of human behaviour related to building energy consumption in the Town Energy Balance (SURFEX-TEB v. 8.2)*. https://doi.org/10.5281/zenodo.4009305

Sorrell, S. (2007). *The Rebound Effect: An Assessment of the Evidence for Economy-Wide Energy Savings from Improved Energy Efficiency*. UKERC. https://ukerc.ac.uk/publications/the-rebound-effect-an-assessment-of-the-evidence-for-economy-wide-energy-savings-from-improved-energy-efficiency/download

Staffell, I., Brett, D., Brandon, N., & Hawkes, A. (2012). A review of domestic heat pumps. *Energy & Environmental Science*, *5*(11), 9291. https://doi.org/10.1039/c2ee22653g

Staffell, I., Brett, D. J. L., Brandon, N. P., & Hawkes, A. D. (Eds.). (2015). *Domestic Microgeneration* (0 ed.). Routledge. https://doi.org/10.4324/9781315697109

Stoecker, W. F., & Jones, J. W. (1982). *Refrigeration and air conditioning* (2nd ed.). McGraw-Hill.

Tornay, N., Schoetter, R., Bonhomme, M., Faraut, S., & Masson, V. (2017). GENIUS: A methodology to define a detailed description of buildings for urban climate and building energy consumption simulations. *Urban Climate*, *20*, 75–93. https://doi.org/10.1016/j.uclim.2017.03.002

Vaishnav, P., & Fatimah, A. M. (2020). The Environmental Consequences of Electrifying Space Heating. *Environmental Science & Technology*, acs.est.0c02705. https://doi.org/10.1021/acs.est.0c02705

Supplementary Material

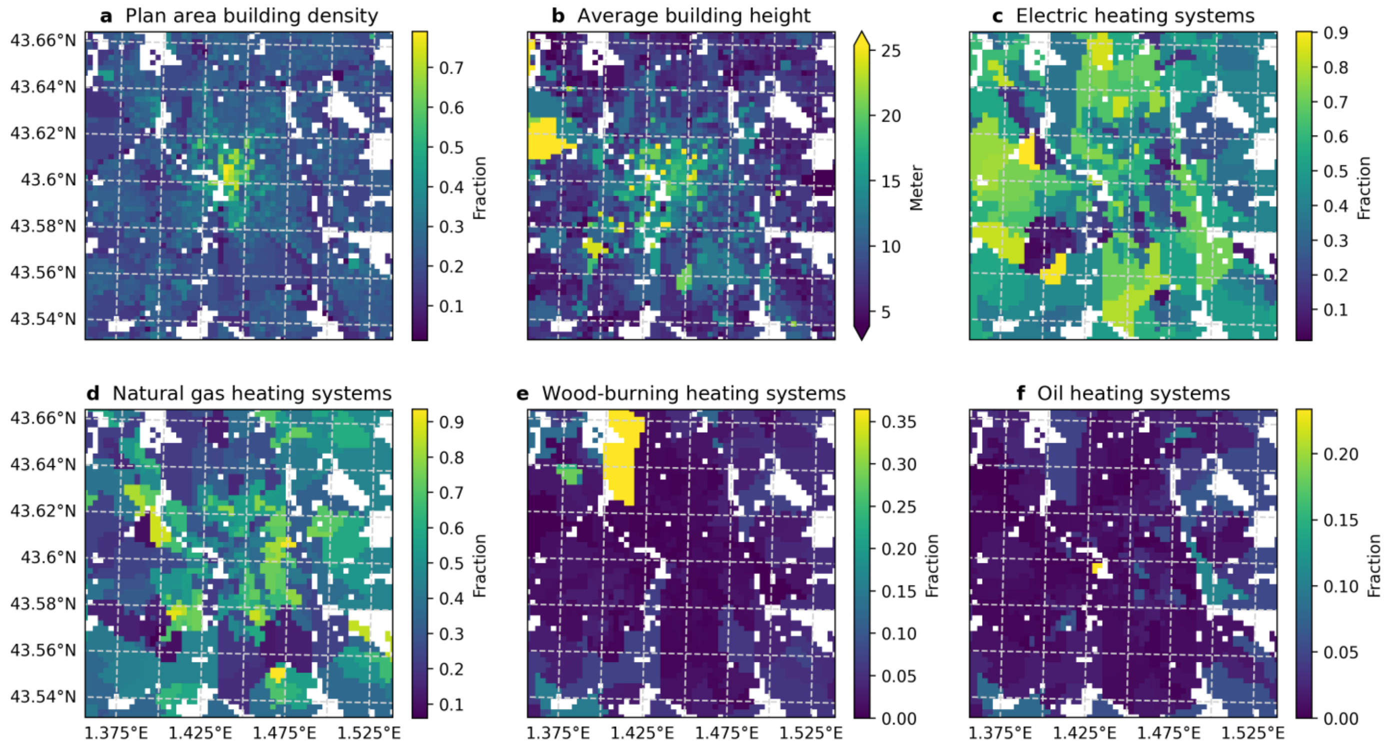

Figure S1 | Input parameters used in TEB.

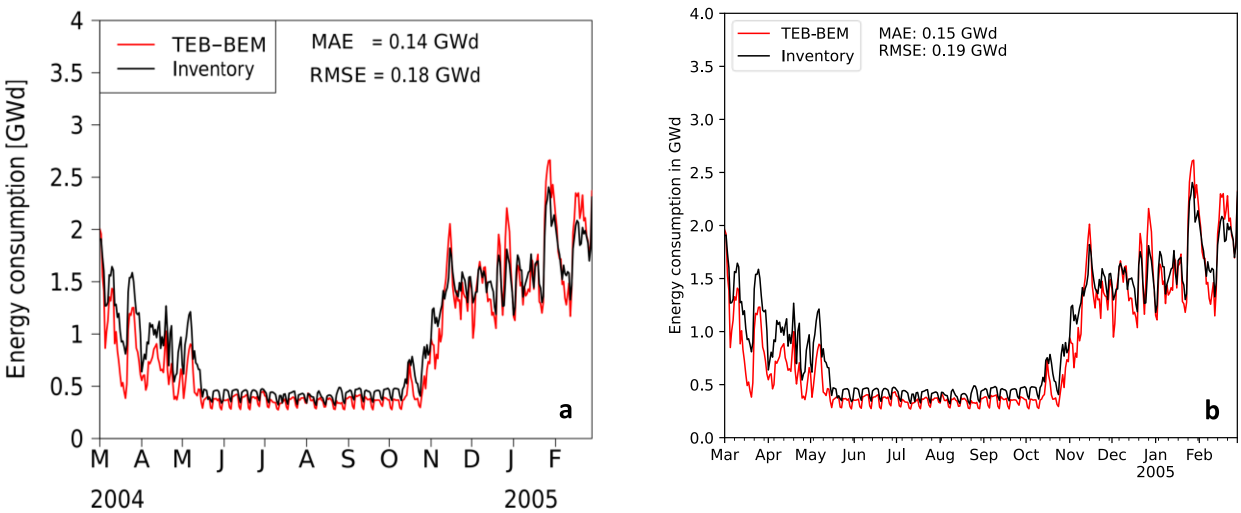

Figure S2 | Evaluation of offline model's baseline scenario. Daily energy use (spanning heating, cooking, lighting, and electrical appliances) within the offline simulation domain from 1 March 2004 to 28 February 2005 with (**a**) the simulation results presented in Schoetter et al. (2017a)'s Figure 6d (licensed under Creative Commons Attribution 3.0) and (**b**) our results closely aligning with their findings. Minor discrepancies of 0.01 GWd in Mean Asolute Error (MAE) and Root Mean Square Error (RMSE) are attributed to updated map inputs used in offline simulations. As noted in Schoetter et al. (2017a), the baseline's energy use is well-represented. The energy consumption during the warm period averages at about 0.4 GWd, revealing a weekly pattern due to decreased occupancy in offices and commercial spaces on weekends. Energy usage during this period shows minimal temperature dependence, reflecting the scarce presence of air conditioners in Toulouse in the summer of 2004.

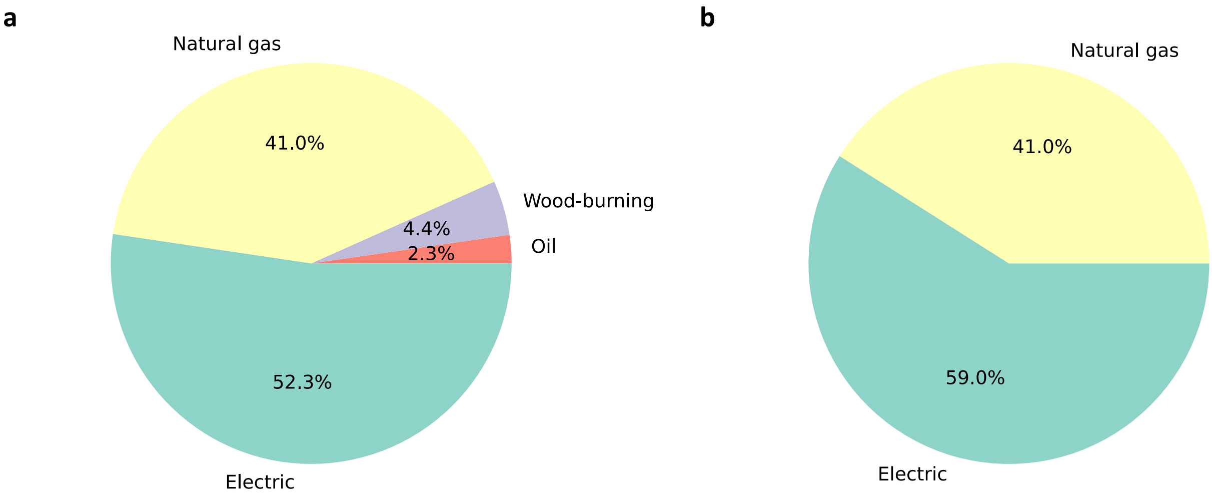

Figure S3 | Proportion of heating fuel types in the domain of investigation. These are shown for (**a**) the entire domain and (**b**) for the dense urban centre of Toulouse (Capitoul).

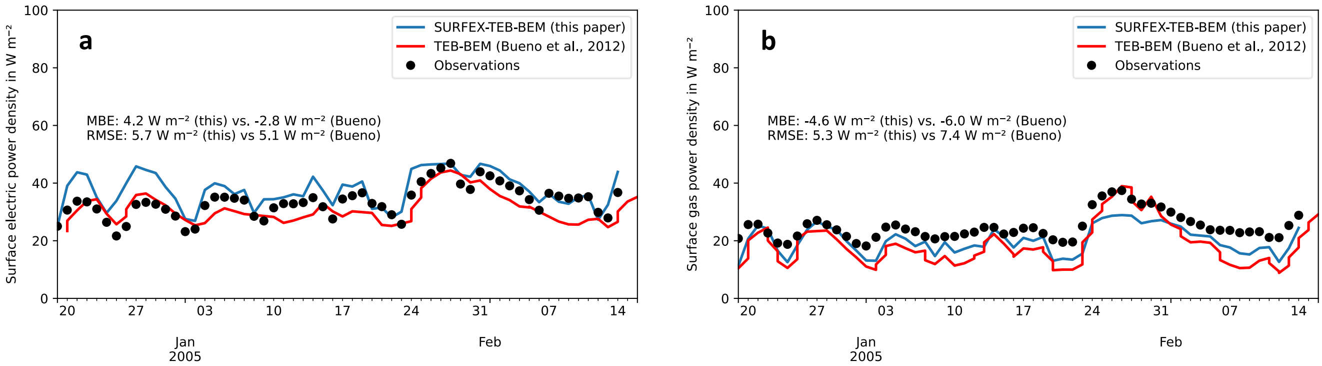

Figure S4 | Evaluation of wintertime daily averaged surface power density in Toulouse's urban centre (Capitoul). The (**a**) electrical and (**b**) natural gas power densities, normalized by urban area, are compared with results from Bueno et al. (2012) and observations. The mean bias error (MBE) and root mean square error (RMSE) are evaluated against observations. Our findings show that the MBE and RMSE values are either lower or on par with those presented in Bueno et al. (2012). Data for plotting TEB-BEM was extracted from Figure 9 in Bueno et al. (2012). A further evaluation for the entire year is shown in Figure S5.

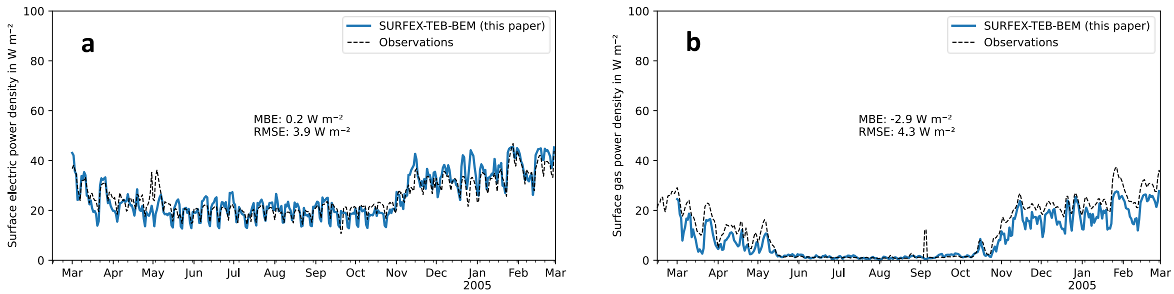

Figure S5 | Evaluation of yearlong daily averaged surface power density in Toulouse's urban centre (Capitoul). The (**a**) electric and (**b**) natural gas power densities, normalized by urban area, are compared with observed values from the dense core of Toulouse. The mean bias error (MBE) and root mean square error (RMSE) are computed against observations.

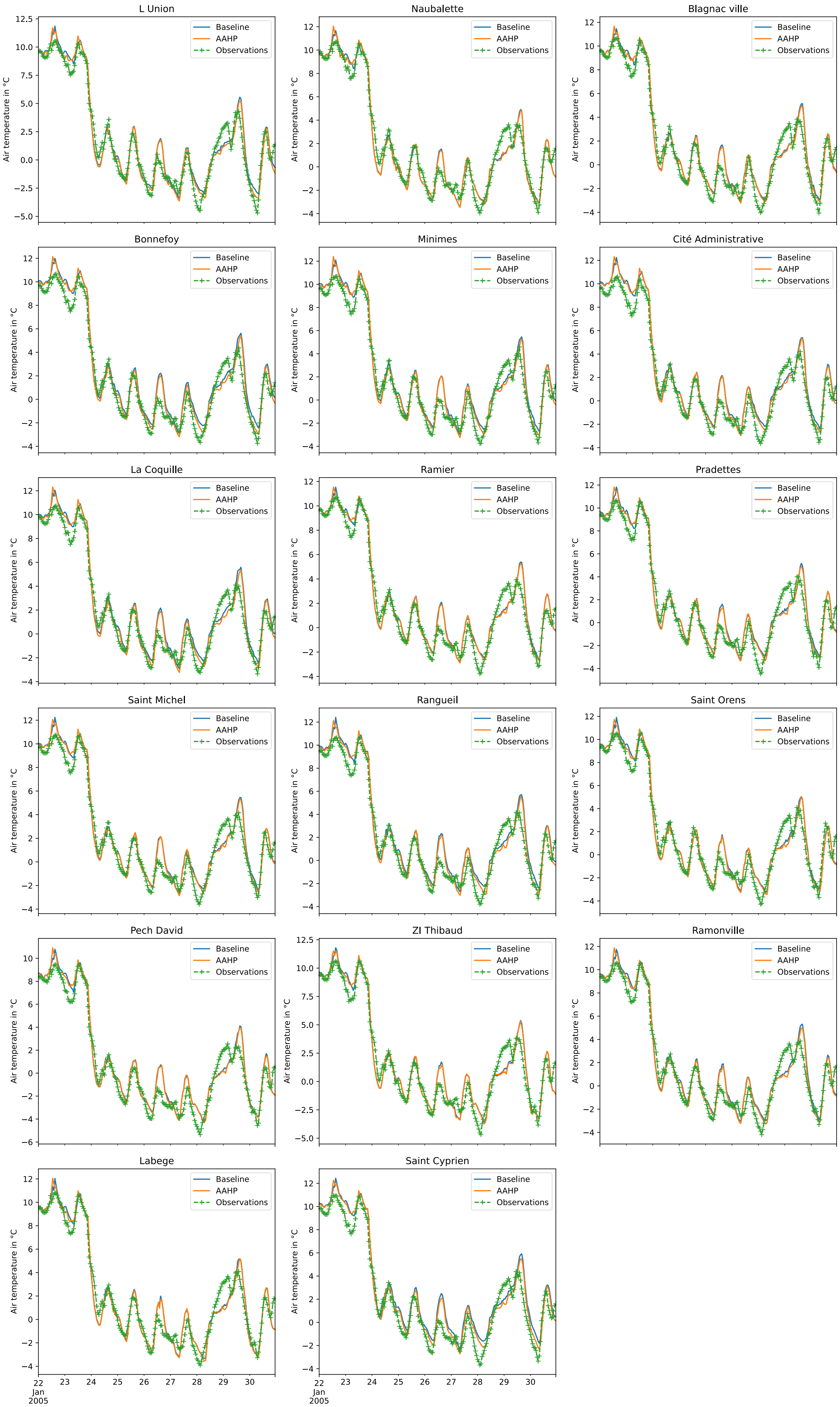

Figure S6 | Comparison of simulated air temperatures. Online simulation results for the baseline and AAHP (RC@2.5) are shown alongside data from 17 observational stations.

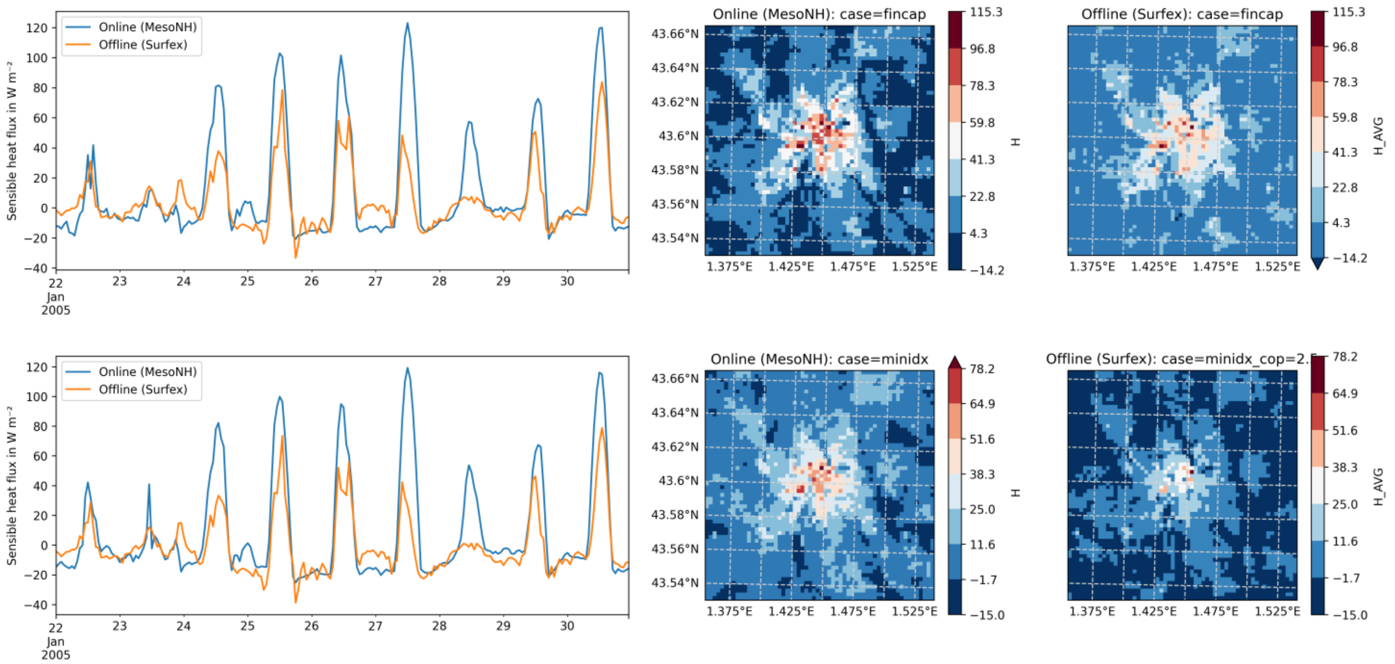

Figure S7 | Comparison of offline and online sensible heat flux during the cold spell period. These are shown for (**a-c**) the baseline and (**d-f**) the AAHP (RC@2.5) scenario.

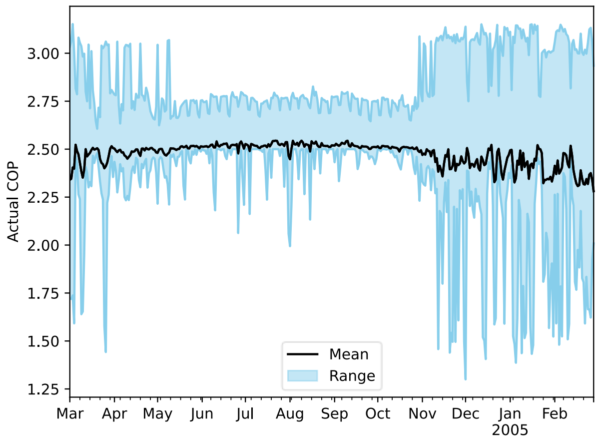

Figure S8 | Evaluation of simulated COP. The RC@2.5 scenario's mean simulated COP (black line) and range (blue shaded area) are shown for the entire domain.